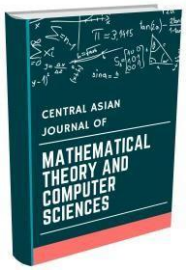

CENTRAL ASIAN JOURNAL OF MATHEMATICAL THEORY AND COMPUTER SCIENCES
https://cajmtcs.centralasianstudies.org/index.php/CAJMTCS
Volume: 07 Issue: 02 | April 2026 ISSN: 2660-5309

Article

A Study of the Effect of High Temperatures on the Thermal Conductivity, Structural and Electrical Properties of the Super-Thermally Conductive Material $Bi_2Sr_2Ca2Cu3O_{8+}\Delta$

Lect. Wisam Shareef Irzooqi*[1]

1. Thi-Qar Education Directorate, Thi-Qar, Iraq, Open Educational College-Thi-Qar
* Correspondence: wisamshareef82@gmail.com

Abstract: The research focuses on the effects observed in the superconducting material resulting from the annealing of $Bi_2Sr_2Ca_3Cu_4O_{10+}\delta$ samples at varying temperatures, starting at 650 °C and increasing by 100 °C on three occasions; that is, in the second case the temperature reaches 750 °C and in the third it reaches 850 °C. In each case, we record the changes in the structure of the material used, as well as their effect on conductivity. The material was prepared in vitro using the solid-state method and synthesised nanoscale. The material was calcined in an oxygen atmosphere to control the phase growth and the structure of the . The results of the X-ray diffraction analysis showed a sequential transition from low-order layers to a well-developed phase, Similarly, the results of the electrical testing showed a marked improvement in conductivity at elevated temperatures, whilst atomic force microscopy (AFM) scans revealed good interparticle bonding within the nanomaterial, The rough surface and distinctive structural morphology at high temperatures demonstrated that the optimum temperature for achieving a superconducting application is 850 °C in the bismuth compound used.

Citation: Irzooqi W. S. A Study of the Effect of High Temperatures on the Thermal Conductivity, Structural and Electrical Properties of the Super-Thermally Conductive Material $Bi_2Sr_2Ca2Cu3O_{8+}\Delta$. Central Asian Journal of Mathematical Theory and Computer Sciences 2026, 7(2), 316-328.

Received: 10th Jan 2026
Revised: 11th Feb 2026
Accepted: 20th Mar 2026
Published: 21th Apr 2026

Keywords: AFM , sold state , ceramic , bismuth , Superconducting , nano size , critical temperature.

Introduction

Superconducting materials possess magnetic and structural properties that set them apart from other materials, and this has made them a subject of interest to researchers and academics, particularly in recent years. Their stable chemistry, satisfactory natural abundance, high magnetic permeability, and distinctive electrical properties, All these properties and characteristics make them suitable for numerous applications, particularly in power converters, as well as in electronic circuits and communications, as they can be manufactured in the form of nanoparticles [1] and can also be used in a wide range of applications, for example in magnetic fluids [2], and they also have practical significance in biomedicine [3]. What makes these materials important is that their particles are influenced by the shape and size in which they are manufactured [4], [5], Currently, nano-sized magnetic oxide particles are being utilised with great interest due to their ideal practical applications, as they are applied and employed in numerous industries [6]. From among the various nanoparticles, materials with superconductivity can be selected for use in vast applications, particularly in electronics, due to their unique and remarkable

properties [7][8], as they are biocompatible and represent an environmentally friendly material used in such applications [9]. As for the preparation of these materials, there are various methods for manufacturing them and reducing them to nanoscale [10] [11]. Among these methods are sol-gel and solid-state synthesis; following synthesis, the materials are calcined in a furnace at various high temperatures, and their structural properties are recorded at each specific temperature [12]. Through these results, the effects of increasing temperatures and other conditions under study can be documented[13]. It is also possible to dop these materials by adding nanomaterials such as Group V elements and others [14] through this doping, numerous changes corresponding to relevant applications can be studied [15], [16]. Superconductivity is one of the most fascinating physical phenomena in solid-state physics, due to its unconventional properties that deviate from the behaviour of materials under normal conditions[17]. Some materials, when cooled to below a few kelvins (in some cases less than 1.5 K), enter into a superconducting state where the electrical resistance of these solid conductors disappears entirely! These materials can carry electric current without energy loss and heat production, placing them in a class of highly efficient materials that have applications such as loss-free power transmission and superconducting technologies [19] [18]. The temperature at (above or below) which this phase transition takes place, known as the critical temperature (Tc), varies from material to material based on their electronic structure and atomic bonding characteristics. So, researchers are forever looking at the periodic table trying to find out different elements or a compound that possess superconducting features in extremely low temperature environment or with more intermediary higher heat. [20] High-temperature superconductors are among the most significant characteristics of these materials, as they conduct current with zero resistance when cooled using substances such as liquid nitrogen. Among the most important of these materials are ceramics, due to their multiple structural layers. An example is bismuth, which is the subject of this research It can form multiple phases when synthesised as a nanoparticle, and its distinctive phases can be obtained through specific laboratory preparation conditions; high sintering temperatures are the most important factor in improving the phases and the aggregation of nanoparticles. In this study, we investigate the effect of different temperatures on the structural and electrical properties of the compound used, as determined by XRD, SEM and AFM analyses, which enable us to identify the optimal performance of these materials.

Ingredients And Preparation Methods

- The Bi-Sr-Ca-Cu-O system compounds were prepared using 99% pure chemicals, such as Bi2O3, bismuth oxide, $Sr(NO_3)_2$, strontium nitrate, CaO, calcium oxide, CuO, copper oxide, and isopropyl alcohol C_3H_3O, which was used as a solvent and helped mix the powders to achieve total homogeneity. During the sintering and annealing operations, oxygen gas (O_2) is used to create a saturated oxidizing environment.
- Tools for preparing samples

The following equipment and supplies were used during sample preparation:

1- G.M.B.A precision balance with an accuracy of 0.0001 g

2- Ceramic boat

3- Small mortar and pestle

4- Electric furnace with a maximum temperature of 1150°C

5- Hydraulic press with a pressing force ranging from 1 to 15 ton/cm²

Once the chemicals had been accurately weighed out according to the specified ratios, each sample was mixed using a ceramic mortar and an agate pestle. Mechanical grinding was carried out for a full hour to ensure complete homogenisation of the components. Isopropanol (C_3H_8O) was introduced as a co-solvent when grinding in order

to prevent the loss of fine particulates during mixing and improve particle homogenisation. After the grinding process was complete, isopropanol from the sample was fully removed by evaporation in an electric oven operated at 750 °C before moving to further thermal steps.

LABORATORY RESULTS FOR THE SYNTHESIS OF THE COMPOUND ($Bi_2Sr_2Ca_2Cu_3O_{8+}\delta$)

- X-RAY DIFFRACTION RESULTS

According to the X-ray diffraction results, as shown in Table (1) and Figure (1), it can be confirmed that annealing temperature significantly influences the crystal phase ratios of Bi-2223 compound. Examination of the primary reaction catalyst reveals an increased proportion (45%) of the secondary phase Bi-2201 at a temperature 650 °C, with a very low percentage for that of Bi2277 (%5), which indicates incomplete in terms large degree [28]. The amount of Bi-2201 phase drastically decreases to 3% while the proportion of the Bi-2212 reaches around 35%, but very small amounts (6%) are found for that synthesis temperature. At 850 °C, however, there is a marked shift in the composition of the Bi-2223 phase, which reaches 85%, whilst the secondary phases decrease to negligible levels (2% for Bi-2201 and 20% for Bi-2212). This marked shift reflects the effectiveness of annealing at 850 °C in promoting the formation of the desired high-conductivity phase and reducing impurities and undesirable phases, confirming that this temperature is the most suitable for preparing the Bi-2223 compound with high crystalline purity. Figure (2) shows the change in the phase ratio of the compound at different calcination temperatures.

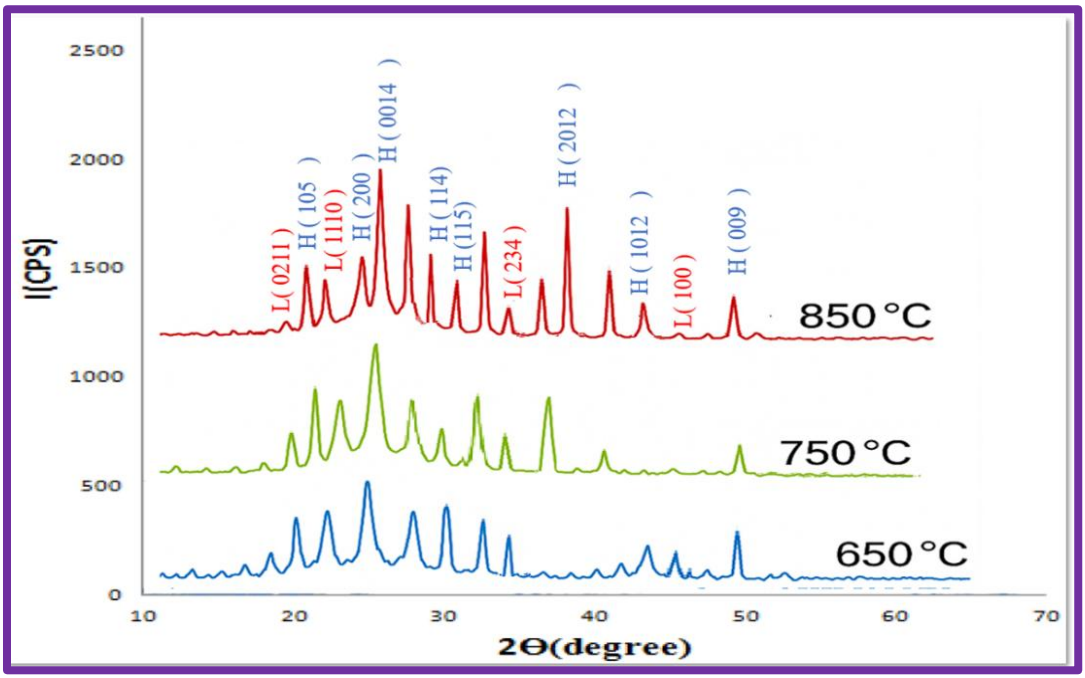

Figure 1. Results of X-ray diffraction for the $Bi_2Sr_2Ca_2Cu_3O8_{+}\delta$ combination at various annealing temperatures.

c/a Ratio	c (Å)	b (Å)	a (Å)	Impurities (%)	Bi-2201 Phase (%)	Bi-2212 Phase (%)	Bi-2223 Phase (%)	Annealing Temperature (°C)
5.62	30.2	5.33	5.37	13	45	28	5	650
5.66	30.6	5.40	5.41	3	3	35	6	750
6.9	37.1	5.44	5.42	2.6	2	20	85	850

Table 1. Structural properties of $Bi_2Sr_2Ca_2Cu_3O8+\delta$ samples annealed at different temperatures.

Table(1) shows that the c/a ratio underwent a marked change with variations in the crystal lattice dimensions, increasing from 5.62 to 6.9 as the c-axis length increased from 30.2 Å to 37.1 Å, clearly indicating that this phase was effectively formed in the third sample. Furthermore, the lattice constants a and b maintained typical values (≈5.4 Å), supporting the structural match with the expected crystal structure of the Bi-2223 compound. Thus, the increase in the c/a ratio to 6.9 is a strong indication of the complete formation of the superconducting Bi -2223 superconducting phase in this sample, compared to the other two samples which exhibited lower c-axis ratios and lower c/a ratios, suggesting that they contain secondary or incompletely formed crystalline phases. Figure (3) shows the variation in the c/a ratio with changes in annealing temperatures.

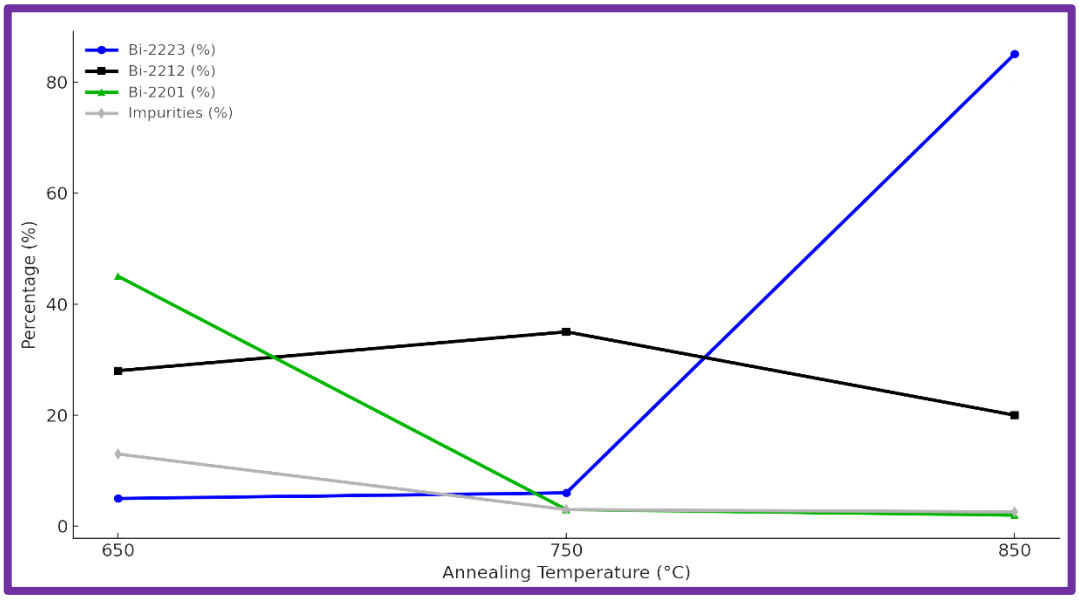

Figure 2. Variation in phase fractions during the synthesis of the compound $Bi_2Sr_2Ca_2Cu_3O8+\delta$ and the impurity content as a function of annealing temperature.

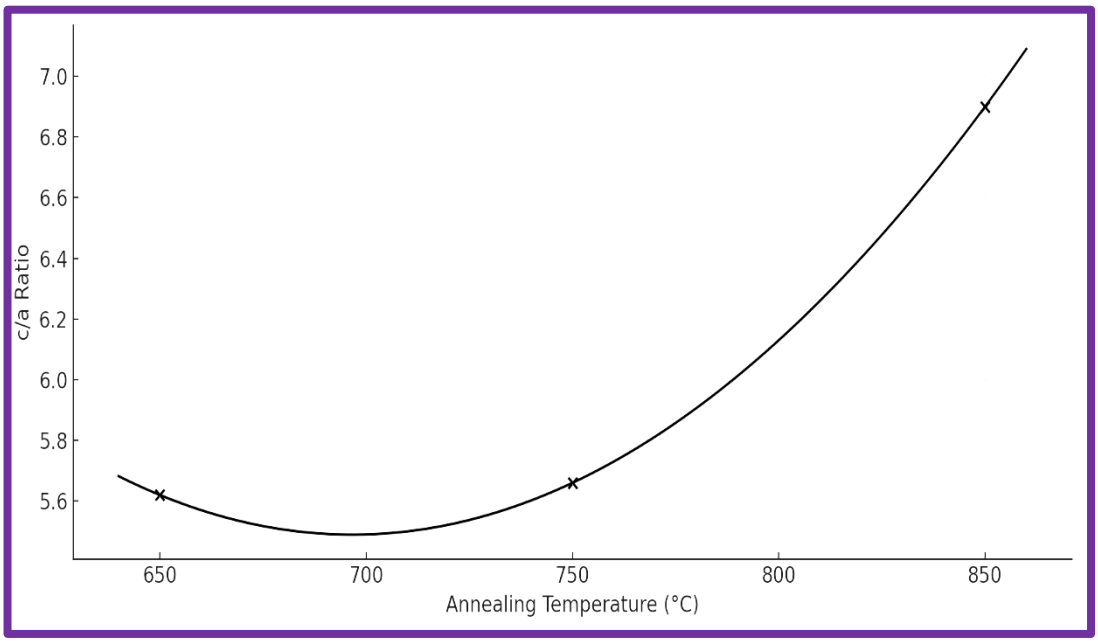

Figure 3. shows the values of c/a as a function of the annealing temperatures used in the preparation of the $Bi_2Sr_2Ca_2Cu_3O8{+}\delta$ compound.

The Debye–Scherrer equation was used to calculate the average crystal size D_sh for the Bi-2223 phase samples; as shown in Table (2) and Figure (4), the sample treated at 850 °C exhibited the highest average crystal size, which reached D_sh = 62.3 nm, indicating good, large-sized crystal growth, reflecting a high degree of internal order in the crystal lattice and the effective and stable formation of the Bi-2223 phase. This improvement can be attributed to the availability of sufficient thermal energy, allowing the atoms to rearrange within the crystal structure and form relatively large crystals. As for the sample treated at 750 °C, recorded an average crystal size of D_sh = 39.5 nm, which is higher than that of the sample treated at 650 °C but still lower than the value achieved at 850 °C, indicating the onset of the target phase formation, albeit with partial crystallisation. Meanwhile, the sample treated at 650°C showed the lowest average crystal size (28.6 nm), suggesting that the temperature was insufficient to achieve uniform crystal growth, and this may be accompanied by the presence of undesirable secondary phases. Based on these results, it can be concluded that 850°C is the optimum temperature for stimulating crystal growth and achieving the highest structural quality of the Bi-2223 phase, which has a positive impact on the structural and, possibly, electrical properties of the samples.

Table 2. Average crystal size of $Bi_2Sr_2Ca_2Cu_3O8{+}\delta$ samples at different annealing temperatures, calculated using the Debye–Scherrer equation.

Average Crystallite Size D_{sh} (nm)	Annealing Temperature (°C)
28.6	650
39.5	750
62.3	850

Figure 4. Crystal size as a function of annealing temperature for samples of the $Bi_2Sr_2Ca_2Cu_3O8+\delta$ compound.

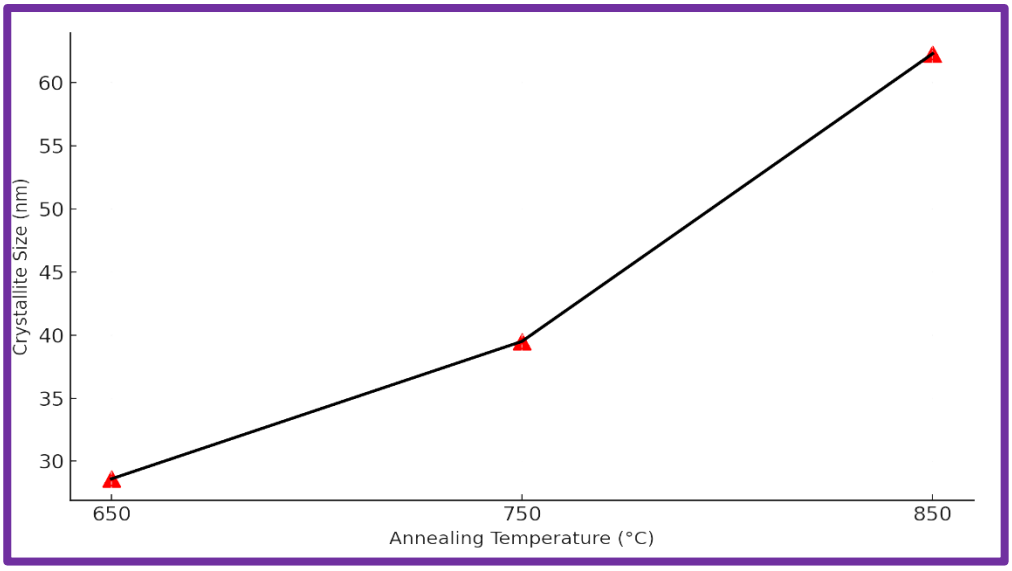

▪ RESULTS ON THE ELECTRICAL RESISTIVITY AND CRITICAL TEMPERATURE OF THE ($Bi_2Sr_2Ca_2Cu_3O_{8+\delta}$) COMPOUND

The relationship between the superconducting transition temperature T_C and the hole concentration p in Bi-2223 phase samples prepared at different annealing temperatures was investigated, with three superconducting transition temperatures identified. The results shown in Table (3) that the sample treated at 850 °C had the highest transition onset temperature (113.8 K) and the narrowest transition range (ΔT_C = 4.2 K), indicating the formation of a high-purity Bi-2223 phase with good structural order. The vacancy concentration in this sample was p = 0.1388, which falls within the ideal range cited by many researchers for maximising Tc in layered materials such as Bi-2223. The sample prepared at 750 °C, on the other hand, exhibited a transition temperature of 110.5 K and a hole concentration of 0.13, indicating the formation of the superconducting phase, albeit to a lesser degree than ideal. Meanwhile, the sample prepared at 650 °C recorded the lowest transition onset temperature of 104.2 K and a hole concentration of 0.12, indicating a low number of carriers (holes) and an incomplete structural transformation. These results indicate a close relationship between the hole concentration p and the superconducting transition temperature T_C, where T_C increases with rising p up to an optimal point, then begins to decrease if the holes exceed the optimum limit. We conclude from this that a temperature of 850 °C is the most suitable for obtaining the best superconducting properties in the Bi-2223 phase. Figure (5) shows the relationship between resistivity as a function of temperature for the compound $Bi_2Sr_2Ca_2Cu_3O_{8+\delta}$at different annealing temperatures, whilst Figure (6) shows the relationship between gaps and annealing temperatures for the compound $Bi_2Sr_2Ca_2Cu_3O_{8+\delta}$

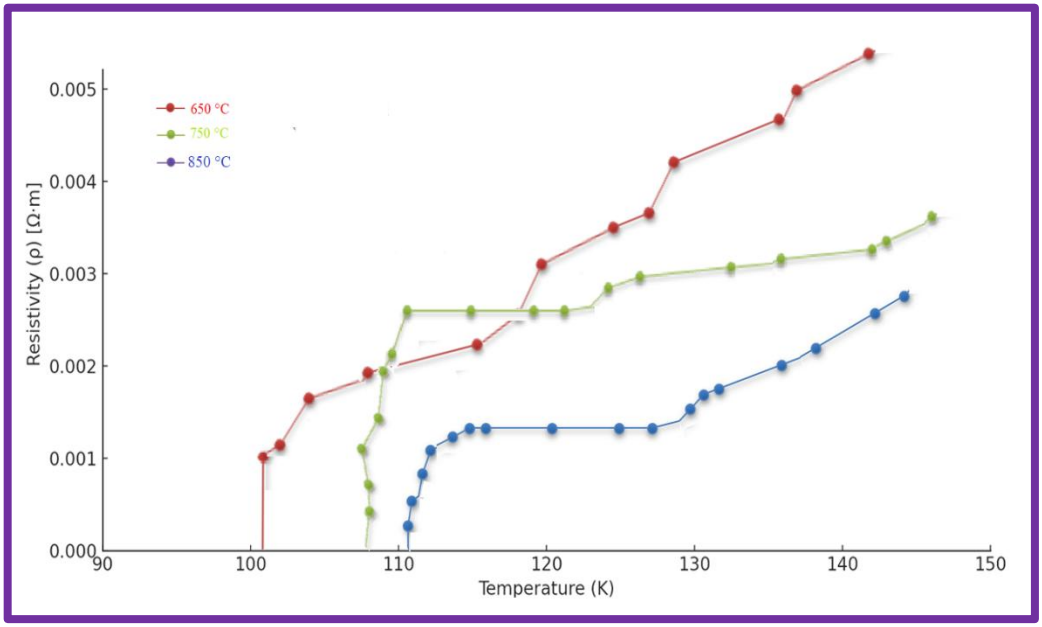

For samples of the compound $Bi_2Sr_2Ca_2Cu_3O_{4+}\delta$ annealed at various temperatures, Figure (5) displays the curves of the relationship between electrical resistance and temperature, showing each sample's transition to the superconducting state.

Table 3. Critical temperatures and pore concentrations for samples of the compound $Bi_2Sr_2Ca_2Cu_3O_{8+}\delta$at different annealing temperatures.

Hole Concentration (p)	ΔT_c (K)	$T_{c\,(off)}$ (K)	$T_{c\,(on)}$ (K)	Annealing Temperature (°C)
0.121	4.7	101.8	104.2	650
0.13011	5.1	107.6	110.5	750
0.13886	4.2	111.2	113.8	850

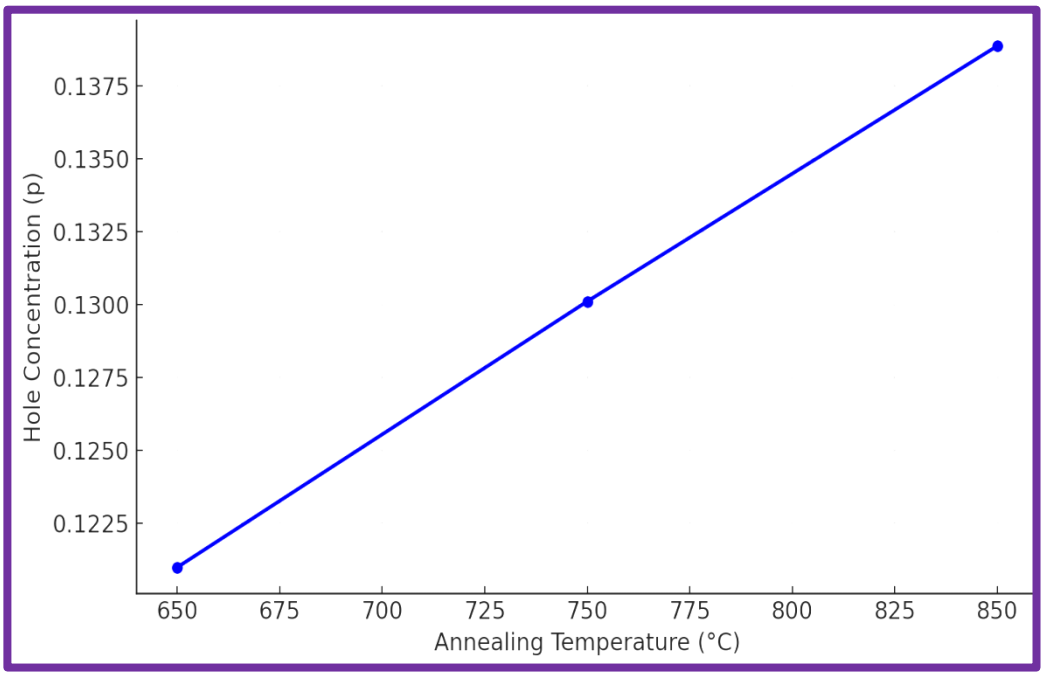

Figure 6. shows the relationship between the annealing temperature and impurity concentration (p) for samples of the $Bi_2Sr_2Ca_2Cu_3O_{4+}\delta$ compound.

- SCANNING ELECTRON MICROSCOPY (SEM) RESULTS FOR THE ($Bi_2Sr_2Ca_2Cu_3O_{8+}\delta$) COMPOUND

A detailed microscopic analysis of the Bi-2223 sample was carried out using a scanning electron microscope (SEM) after annealing at three different temperatures, with the aim of studying the effect of heat treatment on the microstructure of the compound and its relationship to its superconducting properties at 650 °C. The SEM images revealed an irregular structure with small, heterogeneous grains and distinct porosity, as shown in Figure (7) This indicates that the thermal energy was insufficient to achieve mature crystal growth, resulting in weak intergranular bonding and the presence of crystalline voids, which explains the reduced superconducting performance and the broadening of the superconducting transition temperature (ΔTc) in this sample. In addition, high porosity can trap impurities or disturb oxygen concentrations that compromise the superconducting electronic pathways. Plate-like crystals with well-defined edges were observed, along with a notable increase in the grain size and homogeneity within samples synthesized at 750 °C sincethis condition indicates an improvement of crystal growth contributing to better formationof more stable Bi-2223 phase. The enhancement in the structural properties results into improve connectivity among grains, consequent more pronounced superconducting transition and marginally higher superconducting transition temperature T_C as depicted on Fig.

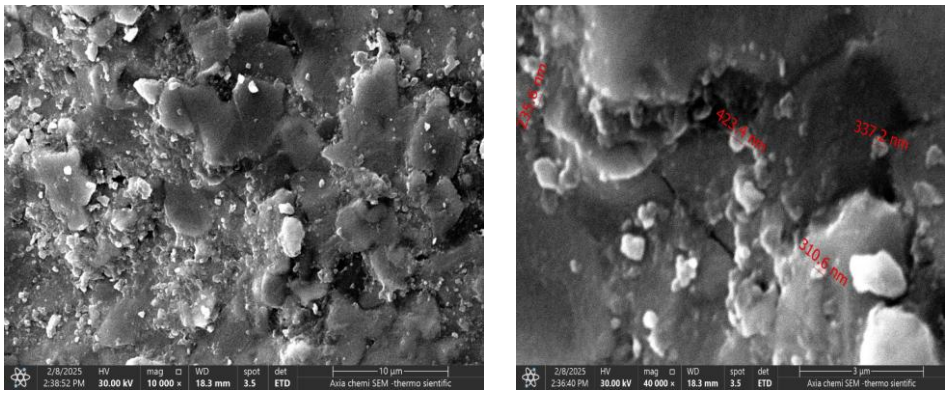

Figure 7. shows a scanning electron microscope image of the compound $Bi_2Sr_2Ca_2Cu_3O_{4+}\delta$ at 650 °C.

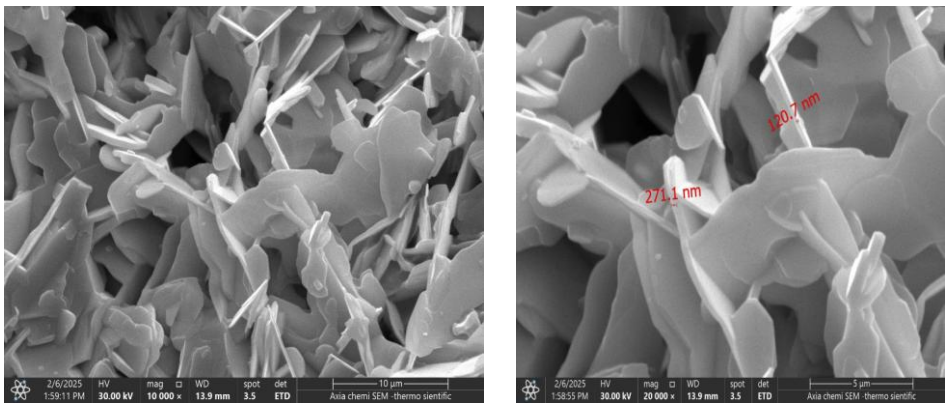

Figure 8. shows a scanning electron microscope image of the compound $Bi_2Sr_2Ca_2Cu_3O_{4+}\delta$ at 750 °C.

As illustrated in Figure (9), the sample annealed at 850 °C displayed more obvious characteristics of advanced crystallisation, with larger and better bounded intergranular grains. This was due to the fact that at high temperature enough energy is provided to reshuffle atoms on a stable crystal lattice leading to a qualitative increase of both grain density and structural bonding. In addition, as the typical feature of textured crystal growth (Textured Growth) revealed that layers melted crystallised along a direction favourable for transporting supercurrent within ab-plane which is considered optimal property in Bi-2223 based materials. Indeed, the structural alignment is perfectly compatible with electrical results being enabled for this sample a higher superconducting critical temperature and narrower transition width. Therefore, results from microscopic examination indicate that the annealing temperature is a crucial parameter for achieving quality of compound's micro-structure and that conducting an excess layer at 850 °C offers optimal condition which aids in developing mature crystal structure enhancing superconducting aspects of $Bi_2Sr_2Ca_2Cu_3O_{8+}\delta$ compound.

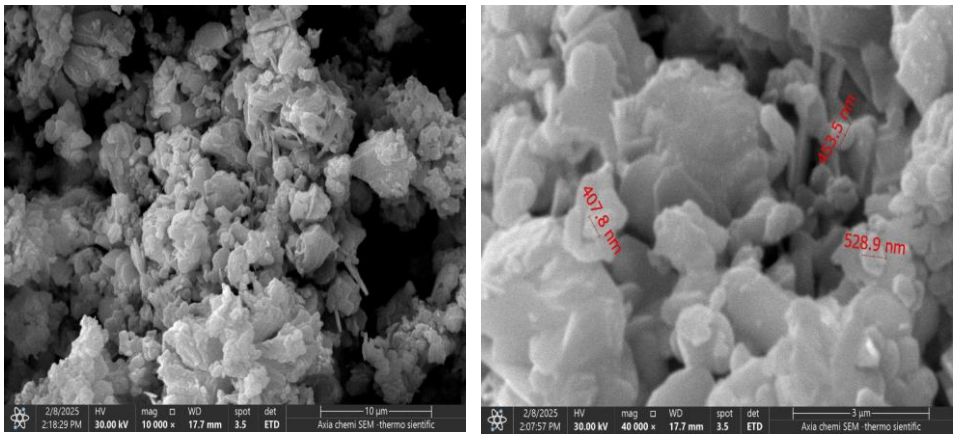

Figure 9. shows a scanning electron microscope image of the compound $Bi_2Sr_2Ca_2Cu_3O_{4+}\delta$ at 850 °C.

▪ RESULTS OF ATOMIC FORCE MICROSCOPY (AFM) ANALYSIS OF THE ($Bi_2Sr_2Ca_2Cu_3O_{8+}\delta$) COMPOUND

Fig. (10) Surface topography of annealed $Bi_2Sr_2Ca2Cu_3O_8 + \delta$ samples taken at three different temperatures were performed with atomic force microscopy (AFM), which display a measure for this high-temperature process, the dealing toward surface structure and also nanoscale roughnesess It was found from the result that roughness values and surface roughness coefficient were significantly different with respect to treatments temperature. The data for surface roughness at 650° also indicates that the average Sa is roughly around 9.8, medium to high but quite irregular and Sdr was ≈96.2%. These values point to a weak atomic rearrangement during annealing, resulting in non-uniformly distributed nanocrystals and incomplete crystal growth neither of which are conducive to good superconducting performance. On the other hand, there was a pronounced improvement concerning surface regularity in the sample annealed at 750 °C as for this group of samples Sa value decreased to around 5.6 nm while Sdr achieved nearly up to double number-72.4 % with more ordered crystalline structure started developing [24]. But the surface topography shows some slight variations, revealing that crystallisation isn't finished yet. On the contrary, for the sample annealed at 850 °C (Fig. 6g), a moderate trend of lower roughness along with smoother surface structure was noted as it resulted in Sa and (Sdr) values to be decreased to only3.2 nmand48.9%, respectively

These values indicate mature crystallisation and a regular distribution of nanocrystalline peaks and voids, reflecting a highly ordered structure closely associated with improved electrical performance and an increase in the superconducting transition temperature (Tc). This behaviour is consistent with the SEM and XRD results, which showed a phase transition to Bi-2223 and clear crystalline stability in the treated samples at this temperature.

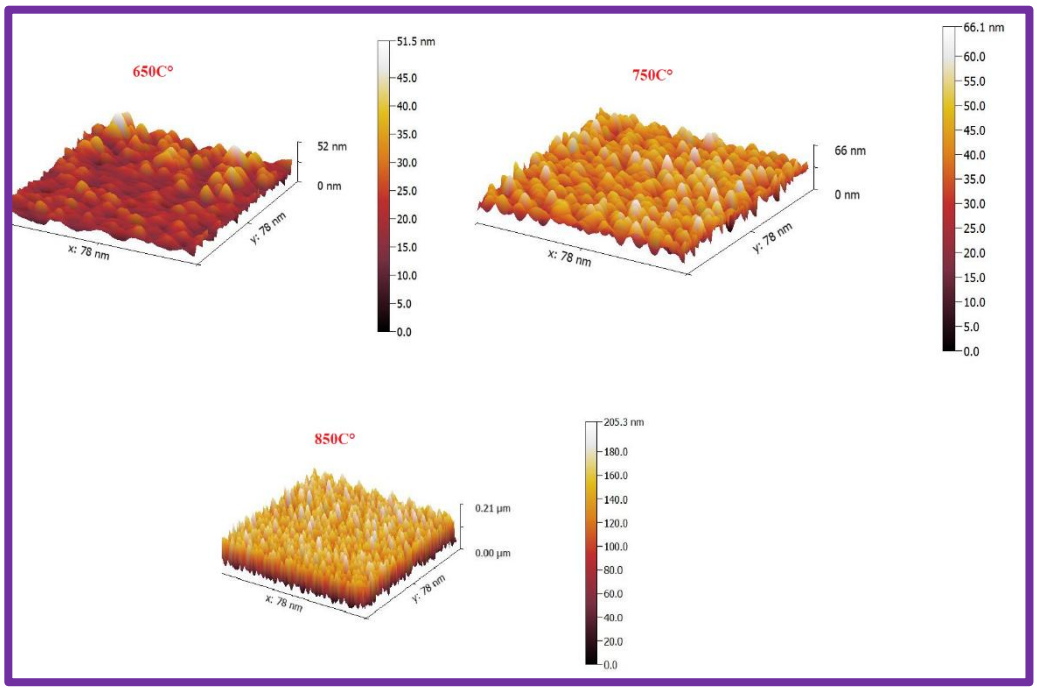

An atomic force microscope image of the $Bi_2Sr_2Ca_2Cu_3O_{4+\delta}$ compound at different annealing temperatures is displayed in Figure 10.

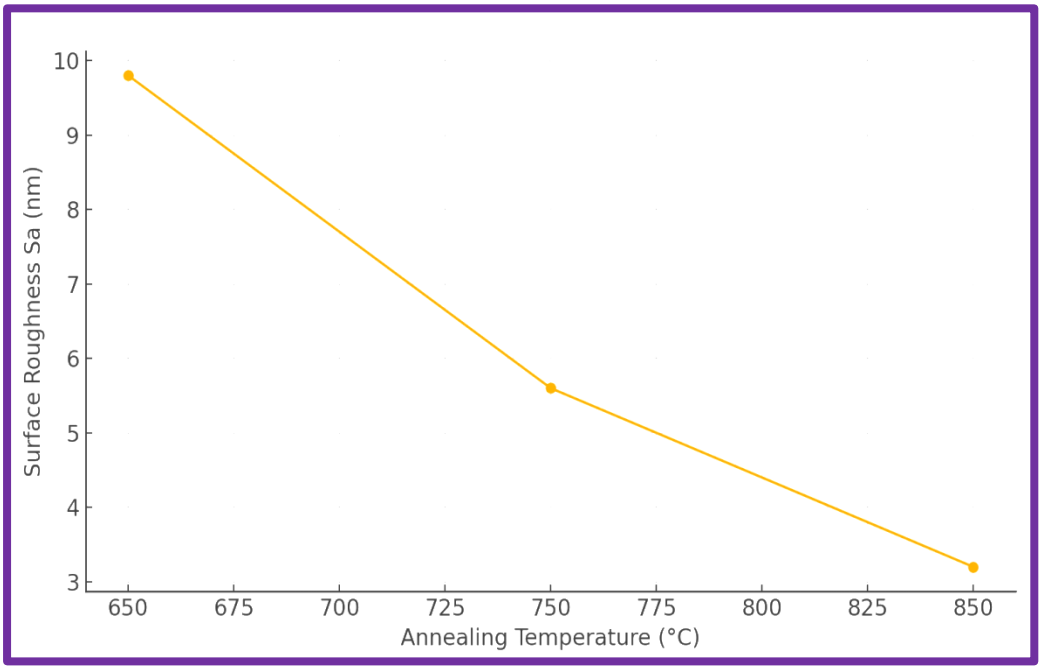

Figure 11. shows the relationship between the annealing temperature and the average surface roughness (Sa) of samples of the $Bi_2Sr_2Ca_2Cu_3O_{8+\delta}$compound, as measured using AFM.

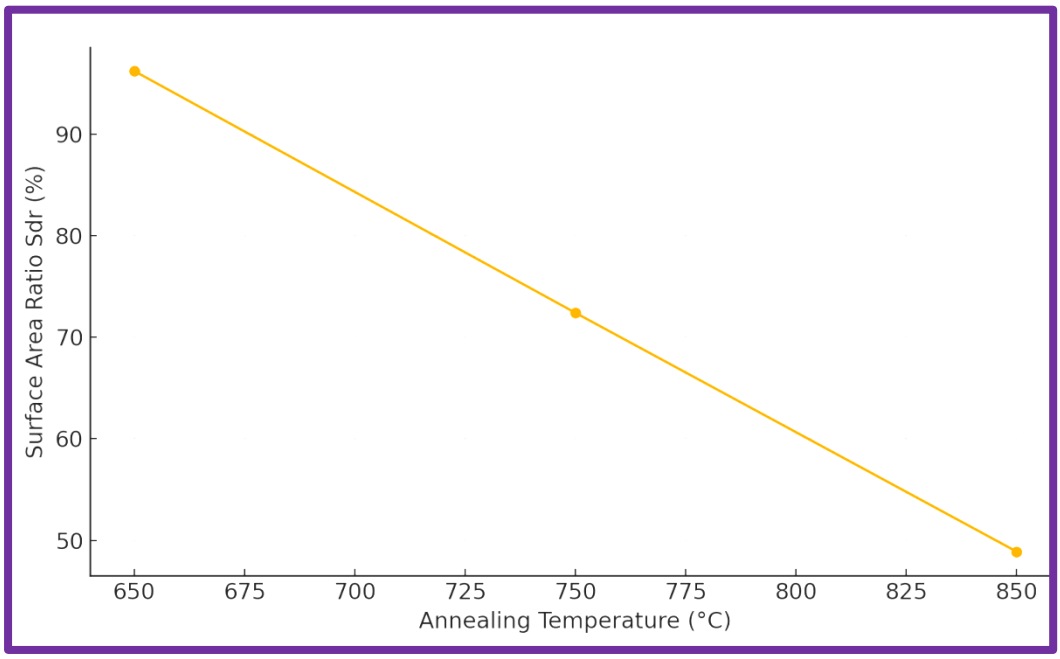

Figure 12. shows the correlation between surface roughness (Sdr) and annealing temperature for $Bi_2Sr_2Ca_2Cu_3O_{4+\delta}$ compound samples as determined by AFM

Conclusion

The results of the analysis showed that high calcination temperatures are the key factor in the excellent growth of the nanomaterial phase; optimal nanoscale dimensions were also obtained. Furthermore, SEM and AFM analysis at high temperatures revealed clear grain size distribution and distinct aggregation of nanoparticles, as well as surface compatibility, resulting in very low electrical loss. A comparison of the three temperatures used for calcining the samples indicated that the highest temperature, 850 °C, is the critical temperature be considered ideal for obtaining a distinctive crystalline nanostructure and high-quality superior conductive properties for the material used in the study.

REFERENCES

[1] Kamerlingh Onnes, H. (1911). Further experiments with liquid helium. C. On the change of electric resistance of pure metals at very low temperatures. IV. The resistance of pure mercury at helium temperatures. Communications from the Physical Laboratory of the University of Leiden, No. 120b.
[2] van Delft, D., & Kes, P. H. (2011). The discovery of superconductivity. Physics Today, 63(9), 38–43.
[3] Essen, H., & Fiolhais, M. C. N. (2011). Meissner effect, diamagnetism, and classical physics – a review. arXiv.
[4] Cardwell, D. A., Larbalestier, D. C., & Braginski, A. I. (Eds.). (2022). Handbook of Superconductivity: Characterization and Applications (Vol. 3). Routledge.
[5] Meissner, W., & Ochsenfeld, R. (1933). Zur Supraleitung bei Zinn. Annalen der Physik, 408(5), 532–540.
[6] Casimir, H. B. G., & Gorter, C. J. (1934). On the interaction between atoms and electrons in superconductors. Physica, 1(4), 306–320.
[7] London, F., & London, H. (1935). The electromagnetic equations of the supraconductor. Proceedings of the Royal Society of London. Series A - Mathematical and Physical Sciences, 149(866), 71–88.
[8] Maxwell, E., & Reynolds, C. A. (1950). Isotope Effect in the Superconductivity of Mercury. Physical Review, 78(4), 477.
[9] Bardeen, J., Cooper, L. N., & Schrieffer, J. R. (1957). Theory of Superconductivity. Physical Review, 108(5), 1175.
[10] Josephson, B. D. (1962). Possible new effects in superconductive tunnelling. Physics Letters, 1(7), 251–253.
[11] Müller, K. A., & Bednorz, J. G. (1986). Possible high-Tc superconductivity in the Ba-La-Cu-O system. Zeitschrift für Physik B Condensed Matter, 64(2), 189–193.

[12] Wu, M. K., & Chu, C. W. (1987). Superconductivity at 93 K in a new mixed-phase Y-Ba-Cu-O compound system at ambient pressure. Physical Review Letters, 58(9), 908–910.
[13] Maeda, H., Tanaka, Y., Fukutomi, M., & Asano, T. (1988). A new high-Tc oxide superconductor without a rare earth element. Japanese Journal of Applied Physics, 27(2), L209–L210.
[14] Ray, P. J. (2015). Structural investigation of $La_{2-x}Sr_xCuO_{4+\gamma}$: Following staging as a function of temperature (Master's thesis). University of Copenhagen, Faculty of Science.
[15] Cmglee. (2012). Periodic table with superconducting temperatures [Image]. Wikimedia Commons. https://commons.wikimedia.org/wiki/File:Periodic_table_with_superconducting_temperatures.jpg
[16] Tinkham, M. (2004). Introduction to Superconductivity (2nd ed.). Dover Publications.
[17] Poole, C. P., Farach, H. A., Creswick, R. J., & Prozorov, R. (2014). Superconductivity (3rd ed.). Academic Press.
[18] Meissner, W., & Ochsenfeld, R. (1933). Ein neuer Effekt bei Eintritt der Supraleitfähigkeit. Die Naturwissenschaften, 21, 787.
[19] Bardeen, J., Cooper, L. N., & Schrieffer, J. R. (1957). Microscopic Theory of Superconductivity. Physical Review, 106(1), 162.
[20] Bardeen, J., Cooper, L. N., & Schrieffer, J. R. (1957). Theory of Superconductivity. Physical Review, 108(5), 1175.